



Characterization of PHB/Clay Biocomposites Exposed to Degradation in an Aquatic Environment

Avilneta Belém de Souza Mesquita^a, Israel Viana da Silva^b, Cristiano José de Farias Braz^b,

Laura Hecker de Carvalho^c , Renata Barbosa^b , Josie Haydee Lima Ferreira Paranagua^a,

Tatianny Soares Alves^{b*}

^aUniversidade Federal do Piauí, Departamento de Parasitologia e Microbiologia, Teresina, PI, Brasil.

^bUniversidade Federal do Piauí, Centro de Tecnologia, Teresina, PI, Brasil.

^cUniversidade Federal de Campina Grande, Centro de Ciência e Tecnologia, Campina Grande, PB, Brasil.

Received: March 01, 2023; Revised: August 19, 2023; Accepted: September 25, 2023

The present work investigates the aquatic biodegradation of poly(3-hydroxybutyrate) (PHB)/nanoclay bionanocomposites containing PP-g-MA as compatibilizing agent. Both pristine and organically modified (Cloisite20A®) montmorillonite clay were used as fillers in different content (1 and 3 wt%). The bionanocomposites were prepared by melt intercalation in a single screw extruder. There after films (50x50x0.5mm) were prepared by compression and assessed by X-ray diffraction. Aquatic biodegradation of the films was appraised by visual inspection, optical microscopy, counting and identification of bacteria. Results proposed that the water of the Parnaíba River in the city of Teresina (Piauí, Brazil) has microorganisms (*Pseudomonas putida* and *Pseudomonas aeruginosa*) capable of degrading these bionanocomposite films, particularly the films with 3 wt% organoclays. Our data indicated the bacteria *Pseudomonas aeruginosa* degraded dexterously all the films. This work collaborates with the preservation of the environment and expands the use of bionanocomposites in expendable items with the development of films with properties favorable to biodegradation in aquatic environments. It is believed that PHB/clay/PP-g-MA films emerge as a promising alternative for the packaging industry.

Keywords: *Aquatic biodegradation, poly(3-hydroxybutyrate), bionanocomposites, environmental preservation.*

1. Introduction

Polyhydroxyalkanoates (PHAs) are biopolymers synthesized by bacteria (*Pseudomonas*, *Alcaligenes*, *Bacillus*, *Azotobacter*, *Rhizium*, *Ralstonia*, *Cupriavidus*, and many others), exhibiting more than 100 monomeric structures. Their mechanical properties vary depending on the length of pendant groups or the distance between ester bonds in polymeric structures. Although always biodegradable, the rate of degradation varies with properties¹. They are still promising biodegradable plastics produced by microbes using waste feedstock², gaining attention for their compostability under environmental conditions³. The technique of producing PHA by fermentation allows the production of several biodegradable products, such as packaging for food⁴ and beverages⁵, films and coatings for packaging⁶, raw material for 3D printing⁷, textile fibers⁸, medical implants⁹, pharmaceuticals and cosmetics¹⁰.

Poly(3-hydroxybutyrate) (PHB) is a polymer with desirable properties, including biocompatibility, reasonable moisture and oxygen barrier properties, and good mechanical properties. Despite its remarkable mechanical properties and biodegradability, this biopolymer has limitations, such as its fragility, physical aging, low crystallization rate, low nucleation density, thermal instability and high production cost. To overcome these challenges, several strategies have been developed, such as heat treatment, blending with materials

from natural sources and synthetic polymers, inclusion of natural fibers or rigid fillers to form reinforced composites, and chemical functionalization¹¹⁻¹⁴.

Researchers report the use of the inorganic nanoparticles as additives to enhance the functionality of polymer. Among these additives are chemically modified clays¹⁵, known as organoclays, which are extensively used in the preparation of bionanocomposites to improve properties such as thermal stability and polymer biodegradation¹⁶. Meanwhile, the use of compatibilizing agents has shown improvements in morphological and mechanical properties due to better distribution and dispersion of the added particles^{17,18}.

Polymeric bionanocomposites are a new class of composites characterized by the combination of natural polymers and inorganic solids and show at least one dimension on the nanometer scale¹⁹. Natural clays, mainly composed of the mineral montmorillonite, form bentonites, a valuable class of minerals for industrial applications due to their high cation exchange capacity and surface area. However, pure bentonites contain impurities that can interfere with these properties and charge dispersion in polymeric matrices, as they are inherently hydrophilic. To solve this problem, clay organophilization was developed, a process that involves the replacement of interlayer inorganic cations by organic quaternary ammonium cations. This serves to increase the distance between layers and reduce hydrophilicity, making it possible to form improved clay/polymer intercalated systems and, in some cases, exfoliated systems^{20,21}.

*e-mail: tsaeng3@yahoo.com.br

Polymer biodegradation occurs when polymers are in a biologically active environment and the biological agents such as bacteria, fungi and enzymes, attack the polymer chains, effectively using them as food and excreting non-toxic small molecules²². Biodegradation is one of the alternatives proposed to manage the amount of plastic waste discarded in the environment²³.

Hydrocarbon-polluted waters provide a suitable environment for the growth of microorganisms that secrete enzymes capable of biodegrading polymers by hydrolysis, making them an alternative treatment for plastic waste²⁴. Adhesion of these microorganisms to the surface of the material is an important step in polymer biodegradation²⁵.

Significant advances in isolation techniques and identification of microorganisms responsible for the metabolism of hydrocarbons have allowed the evolution of scientific research, making available a list of data on microorganisms that degrade hydrocarbons. The literature presents a large group of fundamental microorganisms for the bioremediation of polluted environments²⁶⁻²⁹.

Volova et al.²⁶ observed that the degree of crystallinity of PHAs remained constant during biodegradation in seawater. They proposed that microorganisms, such as *Enterobacter* species, *Bacillus* sp and *Gracilibacillus* sp, could equally disintegrate both amorphous and crystalline phases. In a subsequent study on microbial degradation of PHA's with different chemical compositions in soil²⁷, thirty-five bacterial species were identified as PHA degraders, with each PHA having specific and common degraders. For example, PHB was degraded by *Mitsuaria*, *Chitinophaga*, and *Acidovorax* genera, as well as *Roseateles depolymerans*, *Streptomyces gardneri*, *Cupriavidus* sp, *Roseomonas massiliae*, *Delftia acidovorans*, *Pseudoxanthomonas* sp., *Pseudomonas fluorescens*, *Ensifer adhaerens*, *Bacillus pumilus*, and *Streptomyces*.

Similarly, Faria and Martins-Franchetti²⁸ found that the biodegradation of PHB in the water river occurred proportionally in both amorphous and crystalline phases, and *Gordonia polyisoprenivorans* actinobacteria was identified as potentially capable of degrading PHB. Sayyed et al.²⁹ also observed that the bacterium *Stenotrophomonas* sp. degraded PBH by more than 85% in liquid culture medium and natural soil conditions.

Given the significance of the aforementioned studies to minimize environmental problems related to the resistance to degradation of polymeric materials, this study aims to evaluate the biodegradation of polymeric bionanocomposites exposed to contaminated water from the Parnaíba River collected after the disposal of waste from a beer factory in the city of Teresina (Piauí, Brazil). For this purpose, bionanocomposites were prepared by melting intercalation in a single-screw extruder, films were prepared by compression, and then X-ray diffraction analyzes were performed. Finally, aquatic biodegradation was evaluated by visual inspection, optical microscopy and identification of bacteria. Consequently, the development of films that present favorable properties for packaging applications, demonstrating accelerated and efficient biodegradation when exposed to aquatic environments, emerges as a viable alternative. Therefore, it is believed that PHB/clay/PP-g-MA films represent a promising alternative for the packaging industry, as they will produce non-degraded waste in reduced dimensions that result in a smaller impact on the environment.

2. Materials and Methods

2.1. Materials

Poly(3-hydroxybutyrate), PHB Biocycle® (FE147 lot number) was used as the polymer matrix supplied by PHB Industrial S/A (São Paulo, Brazil) in powder form with MFI equal to 40g.10min⁻¹ (ASTM D 1238, 190 °C/2.16 kg), molar mass of 524.000 g.mol⁻¹, and melting point between 170 and 180°C.

Maleic anhydride grafted polypropylene (PP-g-MA) Polybond™ 3200 supplied by Chemtura Indústria Química (São Paulo, Brazil) was used as compatibilizing agent and to improve the dispersion and distribution of selected clays within the polymeric matrix, as previously suggested^{17,18}. It contains 1 wt% maleic anhydride, MFI = 115g.10min⁻¹ (ASTM D 1238, 230 °C/2.16 kg), density (at 23°C) = 0.91 g.cm⁻³ (ASTM D 792), and melting point = 160-170°C (DSC).

Two different clays were used: (i) a pristine sodium montmorillonite clay (NAT), with specific gravity of 2.86 g.cm⁻³, cation exchange capacity (CEC) equal to 92.6 meq.100g⁻¹, and basal interplanar distance (d_{001}) of 1,17 nm; and (ii) an organically modified montmorillonite clay (ORG), Cloisite 20A, with specific gravity of 1.77 g.cm⁻³, CEC = 95 meq.100g⁻¹, and basal interplanar distance (d_{001}) equal to 2,42 nm. This is a Na⁺-montmorillonite, chemically modified with dimethyl dihydrogenated tallow quaternary ammonium chloride. Both clays were supplied by Southern Clay Products, Inc. (Texas, USA).

The microorganisms involved in the biodegradation tests were the autochthonous ones present in the waters of the Parnaíba River collected after the treated waste discarded from the beer factory in Teresina (Piauí, Brazil) were used as source of microorganisms.

Plate Count Agar (PCA) was used for plating and counting microorganisms and Nutrient Agar was used for bacteria isolation as proposed by Atlas³⁰. A commercial earthworm humus Verdeforte (São Paulo, Brazil) was used as an initial source of carbon.

3M Petrifilm Aqua Heterotrophic (São Paulo, Brazil) membranes were used to quantify the bacteria present in the water of the Parnaíba River, and Cetrimide Agar from Difco™ (New Jersey, USA) was used to identify the bacteria present in biodegradation.

2.2. Bionanocomposites films composition process

The polymer matrix of PHB and compatibilizer (PP-g-MA) were oven dried at 60 °C for 12 h. The compositions containing 1 and 3 wt% of pristine (NAT) or organomodified (ORG) montmorillonite clay, and 2.5wt% of compatibilizer (PP-g-MA) were mixed together with the PHB by manual barrel finishing and then processed in an AX Plastic (São Paulo, Brazil) model Lab16 mono-screw extruder at a screw speed of 50 RPM with a temperature profile of 160, 165, and 175 °C (for the 1st, 2nd, and 3rd zones, respectively). All systems were extruded, cooled in water at room temperature, and granulated at the end in according to previous work³¹. For comparison purposes, pure PHB was prepared under the same conditions.

Posteriorly films measuring 50x50x0.5 mm and approximately 6g of different compositions were molded by compression in a hydraulic press model MH-08-MN from MH Equipamentos (São Paulo, Brazil) operating at 185°C for 20 seconds under a compression force of 4 tons.

2.3. Biodegradation test

The analysis process was carried out followed the previously proposed methodology²⁸. The films were placed in flasks containing water from the Parnaíba River.

Initially, the hummus was sterilized at a temperature of 170°C for 3 h and served as a carbon source. The bacteria these were added to 225 ml of liquid medium and 1.2 g of sterilized earthworm humus in a Backer. All beakers sealed in aluminum foil were kept in a bacteriological oven at 35°C. After the five-day incubation period, the films were immersed horizontally in the liquid medium and remained for withdrawal regular time periods (20, 40, 60 and 80 days) under the same control conditions.

2.4. X-Ray diffraction

X-ray diffraction is considered the most suitable for determining crystalline phases, basal interplanar distances of nanosystems, and the type of structure acquired by nanocomposites³². The films of bionanocomposite were characterized by X-ray diffraction in a Shimadzu XRD 6000 diffractometer (Japan), using Cu K α radiation ($\lambda = 1,5418 \text{ \AA}$), voltage 40 kV, 30 mA, 20 scan from 1.5° to 30° and scan speed of 2° min⁻¹. The relative crystallinity of the samples was quantitatively estimated by calculating the relative peak intensity, using the Origin 2018 software (OriginLab - Northampton, USA)³³.

2.5. TGA analysis

Before and after the biodegradation test, all films were analyzed by TGA technique in equipment SDT Q600 V20.9 Build 20 (TA Instrument), operating at a heating rate of 10°C·min⁻¹ from room temperature to 585°C under argon gas flow of 100 ml min⁻¹. It used about 5 mg of samples.

2.6. Visual inspection

The macroscopic changes observed on the biodegraded films surfaces were visually analyzed and registered by photos taken with a 13MP resolution camera with Carl Zeiss lenses operating with a 2.0/f aperture, 1/3" sensor, and maximum resolution.

2.7. Optical Microscopy (OM)

The surface changes in each biodegraded film were captured under a microscope. MEDILUX optical microscope, operating with 4x magnification (40 μm) and a Digital AM SCOPE MU 14 MP camera.

2.8. Bacterial count

The quantification of the total heterotrophic microorganisms present after each extraction period present in the waters of the Parnaíba River was performed using a 3M Petrifilm Aqua Heterotrophic membrane. From each system 1mL of the liquid medium was sown in Petrifilm membranes. After plating the water sample from the biodegradation systems, was followed for approximately 60 seconds to homogenize the liquid medium next to the plate in a stomacher. The Petrifilm membranes were then placed in sterile plates and kept in an oven for 48 h at 35°C. Afterwards the small red spots which appeared in the plaque were counted following the division

of the quadrants contained in the plate. In calculating of the counts, the value expressed in colony forming unit (CFU) per mL was determined, considering the dilution used³⁴.

2.9. Identification of bacteria in the biodegradation test

Water samples were collected with sterile pipettes and seeded on Brain Heart Infusion (BHI) Agar plates from Difco, with the aid of a Drigalski loop. The colonies of bacteria isolated in the plaque were seeded in the BHI broth. The media were incubated at 37°C for 48h to promote bacterial growth. The procedure for identifying the bacteria present in the test was performed at each removal of the films at 20, 40, 60, and 80 days of incubation. After the isolation in the pure culture, each sample was submitted to the Gram staining technique in differential media for the identification of Gram-positive and Gram-negative bacteria. Subsequently, specific biochemical tests were performed for each isolated genus, following previous recommendations³⁵. In order to confirm bacterial identification, as a result of the difficulty in identifying some species, the samples were analyzed by automation at the Central Public Health Laboratory of Piauí (LACEN) and Med Imagem (Teresina, Brasil).

2.10. Biofilm analysis by *Pseudomonas aeruginosa*

At each removal period, the films were washed with sterile deionized water and placed on a sterilized Petri dish with the aid of a swab and/or platinum cable. The material was sown in BHI broth and cultivated in a bacteriological oven at 37°C for 48h. Then, the sample was seeded on Cetrimide Agar (Difco) using the exhaustion technique and cultivated in a greenhouse under the same bacteriological conditions³⁶. In order to confirm the presence of *Pseudomonas aeruginosa*, samples identified as gram-negative non-glucose fermenting bacilli that formed yellowish-green, brownish or non-pigmented colonies with a fruity odor on Cetrimide Agar were subjected to other biochemical tests, such as the oxidase test, growth at 42°C, alkalinization of acetamide, denitrification of nitrates and motility.

3. Results and Discussion

Films of neat PHB and of bionanocomposites compatibilized with 2.5 wt% PP-g-MA: 1 and 3 wt% natural clay (PHB/NAT1 and PHB/NAT3), with 1 and 3wt% organoclay (PHB/ORG1 and PHB/ORG3) incubated for up to 80 days were analyzed aiming at evaluating the biodegradation by bacteria present in the Parnaíba river.

3.1. X-Ray diffraction

3.1.1. Pristine and organoclay

Diffractograms of pristine montmorillonite clay (NAT) and organophilic clay (ORG) are present in Figure 1. X-ray diffraction showed that a more intense peak at $2\theta = 5.90^\circ$ and basal spacing (d_{001}) of 1.48nm was observed for the pristine clay (Figure 1), in agreement to the literature^{37,38}. Peaks present at 17.37°, 19.8°, 21.95°, and 28.84° suggest that pristine sodium montmorillonite clays having well-organized regular lamellae.

When an organic molecule is intercalated among the galleries do the clay layers forming an organoclay, basal spacing increases. This increase in basal spacing varies with the type, concentration, and orientation of the surfactant employed, as well as the method used for the organoclay preparation^{32,39}.

In the diffraction pattern of the modified clay shown in Figure 1, a diffraction peak with maximum intensity at $2\theta = 3.34^\circ$ is observed related to the basal distance d_{001} of the organophilic clay equal to 2.47 nm. A second peak of lesser intensity is observed around $2\theta = 7.10^\circ$ related to the basal distance d_{002} of 1.21 nm. Similar 2θ values related to d_{001} and d_{002} distances for organophilic clay (Cloisite 20A) were previously reported⁴⁰.

3.1.2. XRD of PHB and its biocomposites

X-Ray diffractograms of the different bionanocomposites containing pristine (PHB/NAT) and organoclay (PHB/ORG) were taken in order to investigate clay dispersion in the polymer matrix as well as structural changes brought by the incorporation of the filler and compatibilizer.

The diffractograms of neat PHB and its bionanocomposites are in Figure 2. Characteristic intense peaks of its crystalline phase of PHB are present at 13.36° and 16.76° corresponding respectively for the (020) and (110) planes. Less intense peaks located at 19.94° , 22.36° , 25.36° , and 27.02° are attributed to planes (021), (111), (121), and (040) respectively⁴¹.

The diffraction peaks of greatest interest in the characterization of bionanocomposites are present in the 2θ region between 1 and 8° , as they indicate the intercalation levels of the polymer chains between the clay lamellae, which allows the formation of different structures⁴².

The increase in basal interlaminar space (d_{001}) of clays within nanocomposites is an indication of the degree of clay dispersion. Thus, the change of d_{001} could be used to indirectly compare the surface compatibility of the silicate/polymer chains in the nanocomposite⁴³⁻⁴⁵. Therefore, due to a better polymer/clay compatibility in the system, more polymer chains are intercalated between the silicate layers, and consequently better results will be reflected in the composite properties^{45,46}.

Our data indicates that only in the PHB/ORG3 diffractogram (3 wt% organophilic clay) there was a lower intensity peak in the region $2\theta = 2.58^\circ$ corresponding to a basal distance of 3.54 nm that is characteristic of the addition of modified clay, and a shift to 2θ equal to 4.83° with basal spacing of 1.83 nm this indicate that there has been a polimeric intercalation between the clay layers^{47,48}. It is believed that the better mobility of short graphitized PP chains towards maleic anhydride (PP-g-MA) in the compatibilizing agent favored the entry of PHB chains between clay layers.

On the other hand, Garrido-Miranda et al.⁴³ developed bionanocomposites based on the blend of PHB and thermoplastic starch TPS plasticized with glycerol and water, loaded with organoclay (Cloisite 15A) and analyzed XRD diffractograms to examine dispersion of clay particles in the bionanocomposite. The authors observed that the characteristic clay peaks were not observed in any of the bionanocomposites with different clay contents (1 and 5wt%), suggesting that there was an intercalation between the layers of clay to the polymer mixture, spreading them completely,

indicating a good affinity between polymers and clay. This absence may represent an exfoliated morphology for the bionanocomposites, which was confirmed by TEM.

Similarly Abbasi et al.⁴⁴ evaluated diffractograms of the polypropylene (PP) and polystyrene (PS) mixture obtained by Friedel-Crafts alkylation reaction in the presence of organophilic clay (Cloisite 15A). The authors observed that the diffraction peak of the PS/clay nanocomposite shifted to lower angles representative of the intercalated morphology. This behavior was attributed to the good interaction between PS chains and organoclay layers. However, the PP/clay nanocomposite did not show intercalation or exfoliation. In this way, there was a better interaction between clay and PS than PP.

The characteristic reflection peaks of montmorillonite clay have disappeared in the bionanocomposites PHB/NAT1, PHB/NAT3, and PHB/ORG1. This result can also be attributed to the effect of the formation of nanoagglomerates and the type of equipment used, a single screw extruder, not favoring an optimized dispersion of the filler.

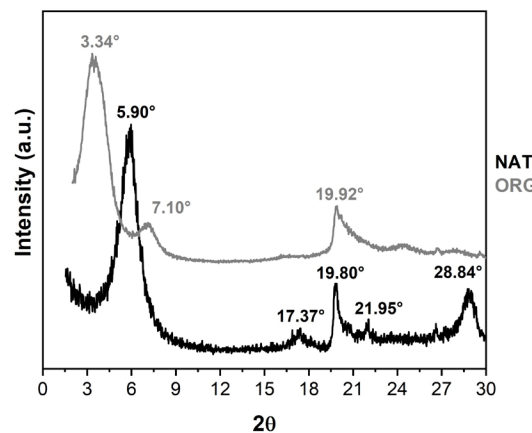


Figure 1. Diffractograms of pristine montmorillonite clay (NAT) and organophilic clay (ORG).

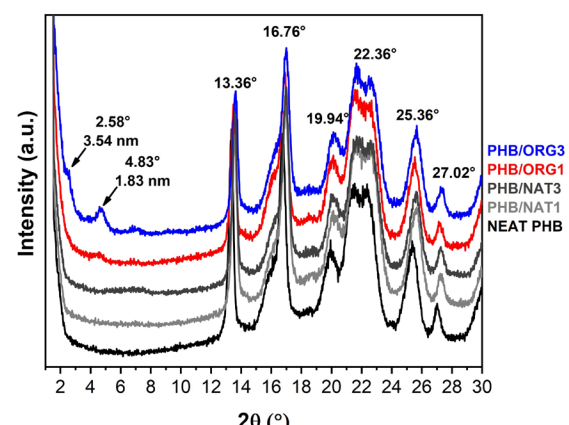


Figure 2. Diffractograms of PHB and its bionanocomposites (PHB/NAT and PHB/ORG).

According to Othman et al.⁴⁶, who analyzed nanocomposites based on a blend of polyamide 6 (PA6) and polypropylene (PP) loaded with organophilic clay (Nanomer 1.30 TC) and PP-g-MA and random polyethylene octene copolymer grafted with maleic anhydride (POE-g-MAH) as compatibilizing agent, the absence of the characteristic clay peak corresponding to d_{001} may indicate that the clay structure was exfoliated and randomly dispersed. Furthermore, the presence of the compatibilizer did not change the dispersion of the organic clay.

On the other hand, Silva et al.⁴⁹, when evaluating nanocomposites of PHB, polyethylene glycol (PEG) loaded with organophilic vermiculite (VMT), observed that the peaks were shifted to smaller 2θ angles compared to the clay peaks, indicating that there was an increase in the interlamellar spaces of the clays due to the intercalation of polymeric chains in the clay layers, and the disappearance of the peaks revealed some degree of exfoliation. They observed that increasing the PEG content reduced intercalation and exfoliation, preventing the PHB chains from entering the organophilic clay layers.

The formation of nanoagglomerates can occur during the nanoparticle production process or when they are incorporated into a polymeric matrix. The direct mutual attraction between nanoparticles via van der Waals forces or chemical bonds is responsible for the aggregation/agglomeration phenomenon⁵⁰. However, strategies such as particle coating, use of coupling agents or compatibilizers or fillers can be employed to prevent or reduce aggregation/agglomeration⁵¹. This situation could remain disadvantageous owing to processing parameters such as extrusion velocity, screw aspect ratio, and other pertinent factors⁵².

No characteristic clay peaks were observed on the bionanocomposites contain pristine clay. This indicates that clay could not have well dispersed, and clay agglomerates were generated. The more hydrophobic clay showed better dispersion due to catalytic activity and chain mobility⁵³, which was confirmed by OM as will be discussed shortly.

Bittmann et al.⁵⁴ investigated PHBV/pristine and organoclay montmorillonite nanocomposites and observed, by XRD, that the best clay dispersion occurred in nanocomposites with 3 and 5wt% pristine clay. However, filler dispersion in these nanocomposites is poor due to large clay agglomerates in the PHBV matrix.

The peak values 2θ and respective basal distances of the clay in the nanocomposites is in Table 1. There is only

a small difference between the angles of the five analyzed compositions, which may mean a discreet intercalation of the clay in the PHB matrix with the aid of the compatibilizer. Zhu et al.⁵⁵ reported that this interaction between the maleic anhydride groups of the grafted polypropylene in the clay galleries leads to intercalation or exfoliation of the bionanocomposite.

It is also observed that the bionanocomposite containing 3 wt% organophilic clay (PHB/ORG3) has the highest d_{001} value. According to Vieira et al.⁵⁶, a displacement of the d001 peak to smaller angles is expected in the bionanocomposite as it is associated with an increase in spacing between the clay lamellae.

From the diffractograms (Figure 2), the calculated crystallinity index (CI) values were 68.2, 68.6, 68.3, 69.3, and 75.2%, respectively, for Neat PHB, PHB/NAT1, PHB/NAT3, PHB/ORG1, and PHB/ORG3. It can be seen that the presence of clay had a negligible impact on the formation of the crystalline structure in PHB. Most films showed a difference of less than 2% compared to pure PHB. However, the PHB/ORG3 film showed an increase in crystallinity (CI) of 10.3% compared to pure PHB, indicating that this particular clay, at this concentration, significantly influenced the crystallization behavior of PHB. This observation confirms with those described in the diffractograms (Figure 2). According to Fambri et al.⁵⁷, the crystallinity of exfoliated nanocomposites tends to be lower than that of intercalated nanocomposites. In exfoliated nanocomposites, the presence of clay lamellae makes chain folding difficult, resulting in the formation of smaller or even imperfect crystalline domains.

3.2. TGA analysis

In the TGA analysis, two parameters were evaluated to assess the thermal stability of the films: the temperature at the onset of thermal decomposition ($T_{10\%}$), which represents the temperature at which a 10% weight loss occurs according to the TG thermograms, indicating the initial decomposition temperature, and the maximum decomposition rate temperature (T_p), determined by the peak of the DTG curves⁵⁸.

TG and DTG thermograms of the films before and after biodegradation under a nitrogen atmosphere are shown in Figure 3 and Figure 4, respectively. The obtained values to TGA analysis before and after biodegradation are listed in Table 2 and Table 3, respectively.

Table 1. Basal interplanar distances of all systems.

NEAT PHB		PHB/NAT1		PHB/NAT3		PHB/ORG1		PHB/ORG3	
2θ	d	2θ	d	2θ	d	2θ	d	2θ	d
-	-	-	-	-	-	-	-	2.49	3.54
-	-	-	-	-	-	-	-	4.83	1.82
13.36	0.662	13.48	0.656	13.58	0.652	13.51	0.65	13.61	0.65
16.76	0.528	16.77	0.529	16.94	0.523	16.87	0.52	16.97	0.52
19.87	0.446	20.18	0.440	20.21	0.439	20.02	0.44	20.23	0.43
22.16	0.400	22.57	0.394	22.55	0.393	22.37	0.39	22.67	0.39
25.74	0.345	25.58	0.348	25.41	0.350	25.51	0.34	25.62	0.34
27.15	0.328	27.24	0.327	27.25	0.327	27.14	0.32	27.35	0.32

2θ in $^{\circ}$; d is the basal interplanar distance in nm.

Prior to biodegradation, all films exhibited a primary stage of decomposition between 214°C and 289°C. This decomposition stage is characteristic of PHB with a mass loss of approximately 95%, as observed in previous experiments^{59,60}. According to Vahabi et al.⁶⁰, the primary mechanism of thermal decomposition of PHB corresponds to the β -elimination of the PHB chains, leading to the formation of crotonic acid, and volatile compounds (dimeric, trimeric and tetrameric).

The applied fillers had a slight impact on the thermal decomposition of the PHB. Both fillers reduced the $T_{10\%}$ temperature by up to 3.53% (PHB/ORG3). The PHB/NAT1 film showed a $T_{10\%}$ value equivalent to pure PHB. Furthermore, the maximum decomposition rates occurred between 269.3°C and 276.6°C (Table 2). It is evident that the presence of mineral fillers also affects the thermal decomposition rate of PHB, as analyzed by the intensity of the peaks present in the DTG curves (Figure 3b).

The films exhibited the following decreasing order of thermal decomposition rate: PHB/NAT3 > PHB/NAT1 > PHB/ORG1 > pure PHB > PHB/ORG3. Thus, it appears that natural clay, at the levels used, favors the decomposition of PHB, while organophilic clay at 3wt% tends to slightly delay this degradation. This behavior can be attributed to the thermal nature of the inert gas inside the PP-g-MA. Despite the low thermal diffusivity, the gas has a higher diffusivity value, suggesting that the gas allows for a greater flow of energy through the thin film, accelerating the degradation³¹.

In addition to presenting values lower than $T_{10\%}$, the films also presented a slight decrease in the peak temperature (T_p) with reductions of 2.17%, 2.36%, and 1.81% for films loaded with ORG1, ORG3 and NAT3, respectively. The NAT1 filler did not significantly affect the $T_{10\%}$ temperature, showing only a 0.29% increase compared to pure PHB.

Table 2. Thermal analysis data of PHB films before biodegradation.

Film	$T_{10\%}$ (°C)	T_p (°C)		Weight loss (%)		Residue (%) at 585°C
		1st	2nd	1st	2nd	
PHB	260.2	275.8	-	96.3	-	1.74
PHB/NAT1	260.4	276.6	419.4	93.0	2.21	2.46
PHB/NAT3	255.6	270.8	440.9	94.3	3.24	2.37
PHB/ORG1	253.6	269.8	412.6	92.7	2.66	3.25
PHB/ORG3	251.0	269.3	389.6	94.5	1.97	2.17

Table 3. Thermal analysis data of PHB films after biodegradation.

Film	$T_{10\%}$ (°C)	T_p (°C)					Weight loss (%)					Residue (%) at 585 °C
		1st	2nd	3rd	4th	5th	1st	2nd	3rd	4th	5th	
PHB	255.9	58.3	-	268.9	-	458.3	0.64	-	74.7	-	9.25	4.82
PHB/NAT1	256.6	39.9	-	270.7	-	454.9	0.62	-	80.5	-	5.47	5.98
PHB/NAT3	256.8	42.3	-	272.4	-	458.8	4.75	-	21.0	-	28.0	27.0
PHB/ORG1	231.2	47.1	219.1	258.0	-	404.4	1.10	4.53	43.1	-	21.4	10.8
PHB/ORG3	277.2	48.6	217.7	269.3	315.9	458.6	3.16	1.92	4.29	15.1	26.7	42.5

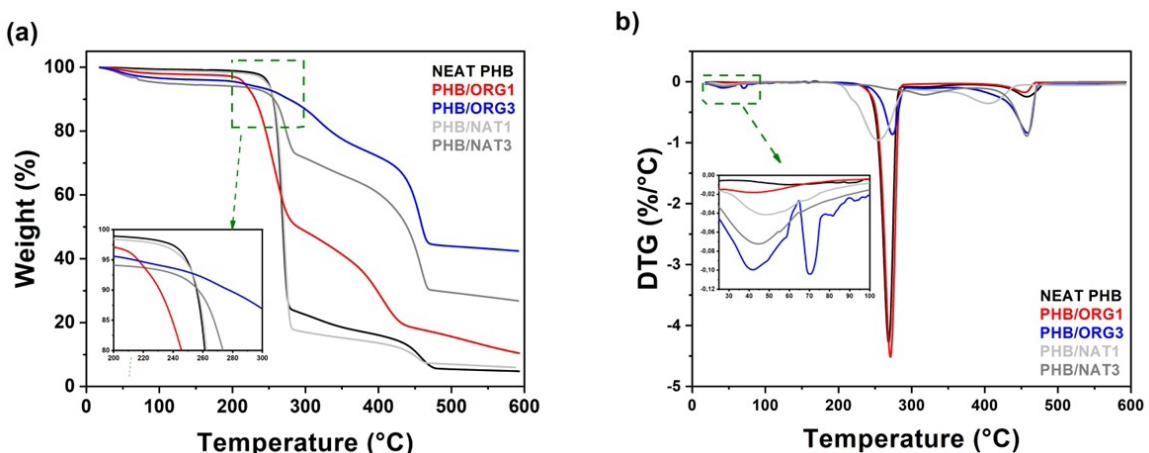


Figure 3. Thermograms of PHB films before biodegradation: (a) TGA and (b) DTG.

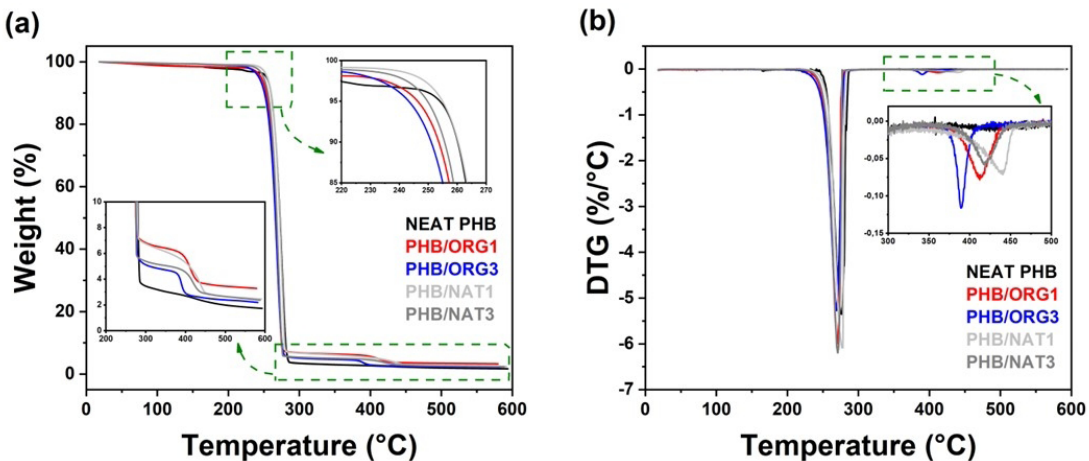


Figure 4. Thermograms of PHB films after biodegradation: (a) TGA and (b) DTG.

The slight decrease in thermal stability contradicts the expected barrier effect of clay, which should restrict the mobility of polymer chains and prevent the release of decomposition products, thereby slowing down the thermal decomposition of the systems³¹. The loss of thermal stability can be explained by the cleavage of the polymeric chains, although the particular minerals must act as thermal insulators⁶¹. The decrease in the $T_{10\%}$ temperature could be attributed to a difference in the amount of surfactant used in the organophilization of the ORG clay, combined with the increase in clay content⁶².

Regarding the residue generated at the end of decomposition previous studies have observed values lower than 2% for the residue of pure PHB at temperatures close to 600°C^{11,14,60}. The presence of inorganic fillers improves the formation of carbon during thermal decomposition. Films with ORG and NAT fillers exhibited higher residue formation, ranging from 24.7% (PHB/ORG3) to 86.8% (PHB/ORG1) compared to pure PHB at 585°C. The increase in residue generated by the ORG filler can be explained by the decrease in oxygen permeability. The formation of a long and convoluted pathway retards oxygen permeation and the release of volatile degradation products. However, the NAT filler seems to be more effective than the ORG filler in improving the thermal stability of the mixture⁶³.

It is also worth mentioning the presence of a second stage of decomposition at high temperatures, ranging from 360 to 460°C, in all loaded films (detail in Figure 3b). The decomposition of this second stage occurred in the following order: 279.7°C (PHB/ORG3), 412.5°C (PHB/ORG1), 419.6°C (PHB/NAT3), and 440.9°C (PHB/NAT1), corresponding to the decomposition of smaller by-products.

This observation can be attributed to the presence of PP-g-MA, which is also present in all films, as well as the aforementioned surfactant agent⁶². The compatibilizing effect improved the dispersion and interaction between the mineral filler and the polymeric matrix. However, it was not able to check the expected thermal resistance of clays for PHB. Furthermore, the presence of the filler may have affected the microstructure of the PHB, leading to the formation of a biphasic system due to the presence of undispersed and poorly distributed particles, as observed in a study on PHB

loaded with TiO₂ by Valle Julianelli et al.⁵⁸. On the other hand, the presence of clays can act as catalysts for the degradative process. This behavior contradicts the findings reported by Pessini et al.⁶⁴ in their study on PLA/PHB blends loaded with organophilic clay (Cloisite 30B).

Silva et al.⁶⁵ analyzed PHB/vermiculite composites and analyzed PHB/vermiculite composites and reported the presence of thermal events between 300°C and 400°C, suggesting the existence of two different polymeric fractions in crystalline structures coexisting between the clay lamellae, which may have influenced the distinct behavior observed in the second degradation event.

When analyzing the effects of biodegradation (Figure 4), it is observed that all films exhibit distinct behavior compared to non-exposed films. A primary stage characterized by the presence of water can be noted, during which the evaporation of free water molecules takes place^{66,67}. The presence of clay reduced the maximum decomposition temperature (T_p) in this stage by up to 11.2°C for PHB/ORG1 and 18.4°C for PHB/NAT1 compared to pure PHB (Table 3). Furthermore, an increase in mass loss is observed with the presence and content of clay in relation to pure PHB. The PHB/ORG3 and PHB/NAT3 films exhibit almost 5 times and 7.5 times more mass loss than pure PHB, confirming the hydrophilic characteristic of the clays⁶⁷.

It appears that the presence of clays affected the characteristic behavior of thermal decomposition of PHB. Films filled with organophilic clay (ORG) exhibit discrete additional stages compared to films filled with natural clay (NAT) and pure PHB film. It is believed that the ORG clay promotes biodecomposition by facilitating a greater accumulation of microorganisms on its surface, resulting in the fragmentation of the polymeric material and requiring a smaller amount of energy for its thermal decomposition. This behavior mainly affected the decomposition step of the ester groups characteristic of PHB, leading to a significantly lower amount of residue at the end of the analysis. According to Fonseca et al.⁶¹, during biological degradation, biofragmentation of polymeric chains occurs, converting them into smaller molecules. Subsequently, the biotic agents effectively assimilate these shorter chains.

This degradation increases the thermal conduction area in the polymeric matrix, facilitating the distribution of heat to a smaller polymeric mass, thus requiring less energy for decomposition during heating⁶⁸.

Consistent with Mamat et al.⁶⁹, the biodegradation can result in the inclusion of various constituents, such as cellular components of bacteria. The presence of these inclusions in PHB results in a black residue, coming from non-volatile carbonaceous materials from bacterial cells.

In addition to clays, the presence of PP-g-MA can influence these results, as reported by Kwon et al.¹⁴. The authors observed that the presence of PP-g-MA mixed with PHB increases the permanence of PHB after biodegradation. They noted that the PHB/PP-g-MA ratio increased from 8% to 11% after biodegradation, suggesting a greater interaction between PHB and PP-g-MA, which hinders enzyme access to the innermost polymeric chains. In the present study, the residue of pure PHB films was almost 3 times greater than non-biodegraded films. A 20-fold increase in residue is observed for PHB/ORG3 and 11-fold for PHB/NAT3.

Films filler with 1 wt% showed similar behavior with almost three times more residue, indicating less interaction with microorganisms during biodegradation.

Lastly, at high temperatures close to 500°C, secondary decomposition of PHB occurs, with the formation of propylene and carbon dioxide as the main products⁷⁰. This decomposition arises from the decarboxylation of primary degradation products, such as crotonic acid, along with minor products including carbon monoxide, ketene, and ethanal⁷¹.

3.3. Visual inspection

Macroscopic analysis was performed on all the films in order to visualize the incorporation of microorganisms through microbial staining, degree of stain growth in the samples, and biofilm formation. Photographs of all the films after exposure periods of 20, 40, 60, and 80 days are shown in Figure 5. In all cases, the same profile of microbial attack was noticed. All films had partially or totally white spots on their surface, indicating that the microorganisms adhered to the surface of the samples, and a biofilm was gradually formed³⁵.

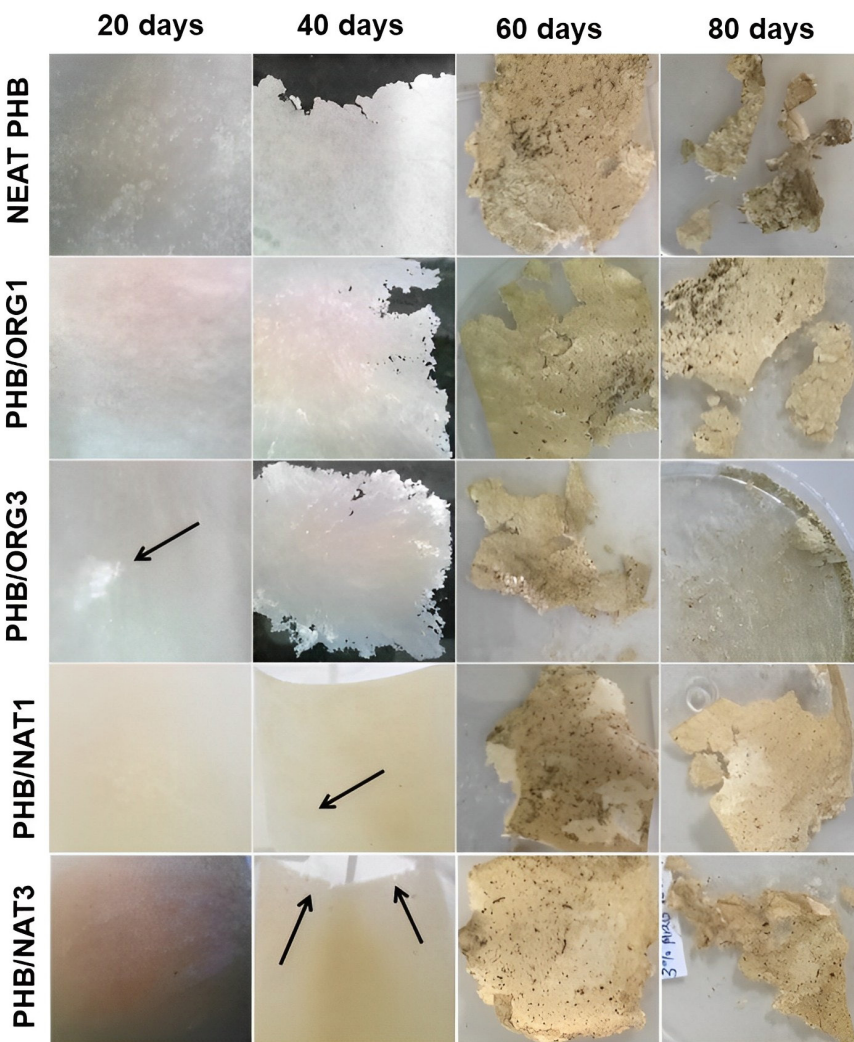


Figure 5. Photographs of the systems throughout biodegradation.

On the 20th day, the PHB film was covered by small spots with no apparent signs of biodegradation. The PHB/ORG1 system showed spot practically all over the film, while the PHB/ORG3 system showed only a small and accentuated spot. On the other hand, the PHB/NAT1 system did not present relevant stains on the film, as opposite to the PHB/NAT3 system, which had a small part of its surface covered by spots.

On the 40th day, biodegradation became more pronounced. The pure PHB films and the PHB/ORG1 and PHB/ORG3 systems experienced more significant degradation as parts of the film were fragmented. However, the PHB/NAT1 system did not show evidence of biofilm formation on its surface. However, it was possible to observe that the transparency was greater at some points on the surface, indicating that the thickness of the film was reduced in these sites. Therefore, suggesting that there was a loss of mass locally⁷², as seen by the arrows in Figure 5. Although the PHB/NAT3 system did not show significant biodegradation as observed in the other films, it is possible to observe some wear on the upper part of the film, indicating that there was some biodegradation.

At 60 days, a biofilm had formed on the surface of all analyzed films. The biofilm formed on the pure PHB sample showed complete adhesion with deposition of humic organic matter. It was also observed that there was a reduction in the surface area of all films, suggesting more efficient biodegradation. However, the PHB/ORG3 system presented greater biodegradation compared to the others. According to Camani et al.⁷³ the Cloisite20A clay used to develop nanocomposites with a PBAT matrix was able to promote an increase in the biodegradation rate, as the increased hydrophilicity of the nanocomposites proved the elevation of sodium ions between the lamellae of the nano clay and promoted an increase in polarity, consequently increasing hydrophilicity, which can increase biodegradation. In addition, a possible increase in surface roughness can generate greater accessibility of microorganisms to the surface of the materials.

At the end of the test (80 days of exposure), all films were more intensely fragmented, and the biofilm formed from the organic deposition was completely adhered to the surfaces. The PHB films and the PHB/NAT1 and PHB/ORG1 systems had similar behavior with the fragmentation of their films. For this period, the PHB/NAT3 system showed a more pronounced reduction with a large loss of mass locally. However, at the end of the test, the PHB/ORG3 system lost the most mass, indicating that this system had the most pronounced biodegradation.

The photographs show that the films underwent changes on their surface, known as biodeterioration⁷⁴, an interfacial process in which microorganisms attack and colonize the surface of the polymer, causing surface modifications by deposition of excreted extracellular material, accumulation of water, penetration of the polymeric matrix with microbial filaments and excretion of lipophilic microbial pigments that modify the polymer's color.

During biodegradation, extracellular enzymes generated by the microorganism break the polymer chains, forming smaller short-chain molecules (oligomers, dimers, and monomers) that are able to cross the semipermeable external bacterial membrane and can be used as sources of carbon and energy. This process is called depolymerization⁷⁵.

In the depolymerization of PHAs, such as PHB, by *Pseudomonas aeruginosa* and *Pseudomonas putida*, several enzymes are produced. Among these enzymes are polyhydroxyalkanoate hydrolases (PHAses), which are responsible for the hydrolysis of ester bonds present in PHA molecules. For example, PHAses can degrade PHB into hydroxybutyrate (HB) monomers or smaller oligomers. Additionally, kinases are involved in the phosphorylation of certain molecules, converting them into their corresponding phosphates, which prepares PHB for the action of PHAses. Finally, reductases are enzymes responsible for the reduction of specific functional groups in PHA molecules, contributing to their degradation and subsequent metabolism⁷⁶⁻⁷⁸. However, in general, these enzymes are not known to cause direct damage to other organisms present in the environment. However, certain factors can influence the behavior of excreted enzymes and indirectly affect other organisms in various ways⁷⁹⁻⁸¹.

3.4. Morphological analysis

The appearance of the surfaces of all films produced before and after biodegradation by bacterial attack was observed by optical microscopy. Indicators used to describe the effects of degradation include surface roughness, crack formation, fragmentation, color changes, and biofilm formation. These changes demonstrate the presence of a biodegradation process under metabolic conditions. Visual changes can be used as an initial sign of microbial attack⁸². The OM and the SEM images of all films before and after 80 days of exposure to the biotreatment are shown in Figure 6 and Figure 7, respectively.

The surface of neat PHB film is rough and shows marks resulting from the compression molding process used to obtain the films. The addition of organophilic clay in bionanocomposites PHB/ORG1 and PHB/ORG3 led to a reduction in film roughness compared to neat PHB, this is probably due to the good adhesion of the nanoparticles to the polymer matrix⁸³. Additionally, PHB/NAT1 and PHB/NAT3 nanocomposites have a rougher surface than the neat polymer, this possibly indicates that the montmorillonite clay in its natural shape creates agglomerates that deposits on the surface of the film. This behavior is also noticed in X-ray diffraction spectra.

After 80 days of biotreatment, the degradation occurs predominantly on the surface of the samples as the enzyme adapts to the stereochemical conformation of the polymer, which then undergoes surface erosion⁸⁴. The roughness of all film samples also increased after these exposure periods, and the deposition of dark spots resulting from biofilm formation is clearly observed. Biofilms may contain microorganisms that produce pigments. Some of these pigments, particularly those formed by specific bacterial strains, are lipophilic and tend to diffuse into the polymer matrix when produced by microorganisms in biofilms⁸⁵.

In addition to the dark spots, all films after exposure period of biodegradation also presented voids and cracks, this indicates that the bacteria contained in the biofilm broke the polymer bonds and possibly consumed the amorphous parts of the polymer matrix. After exposure, the bionanocomposite PHB/ORG3 was extensively biodegraded and its structure was completely modified and compromised, which made it impossible to describe in detail the action of bacteria on this film.

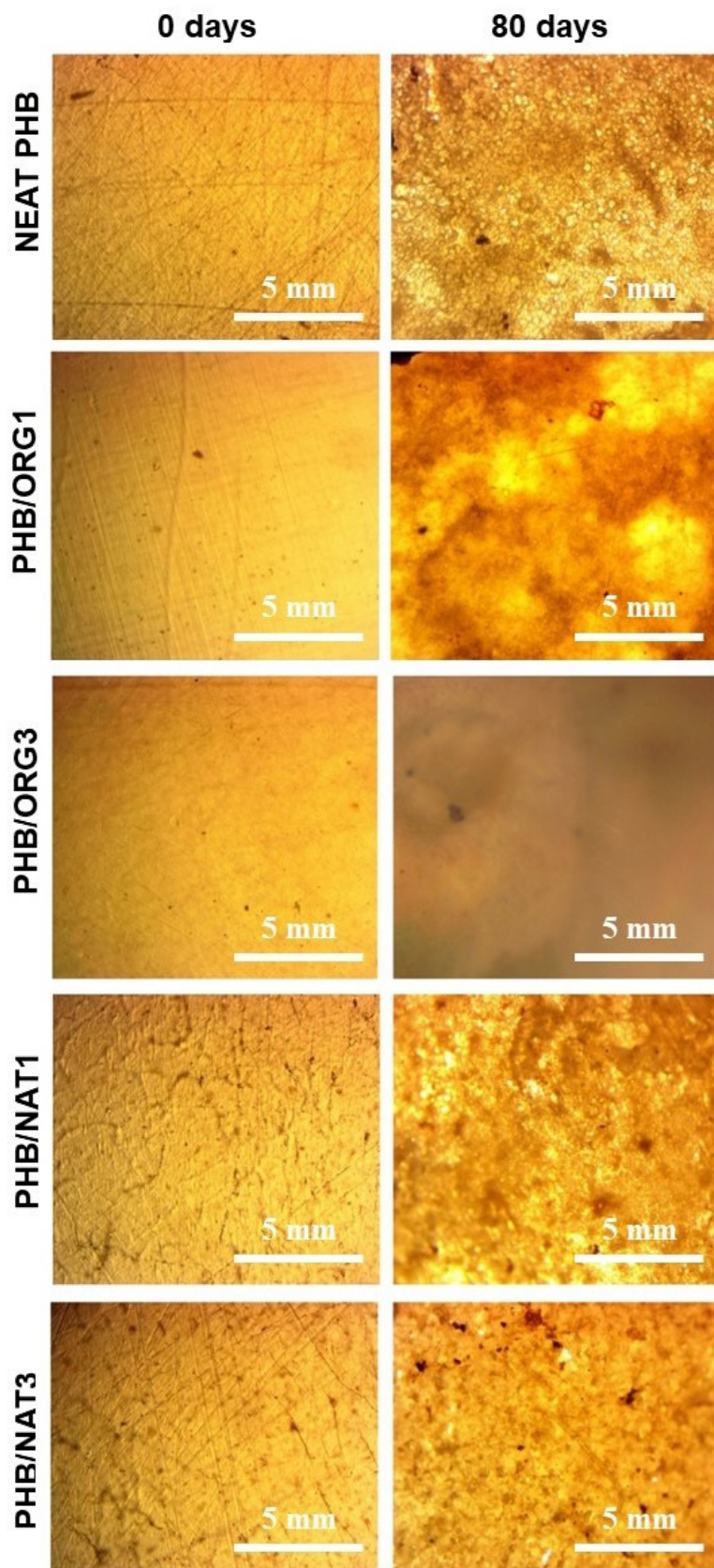


Figure 6. Optical micrographs of the films before and after biodegradation.

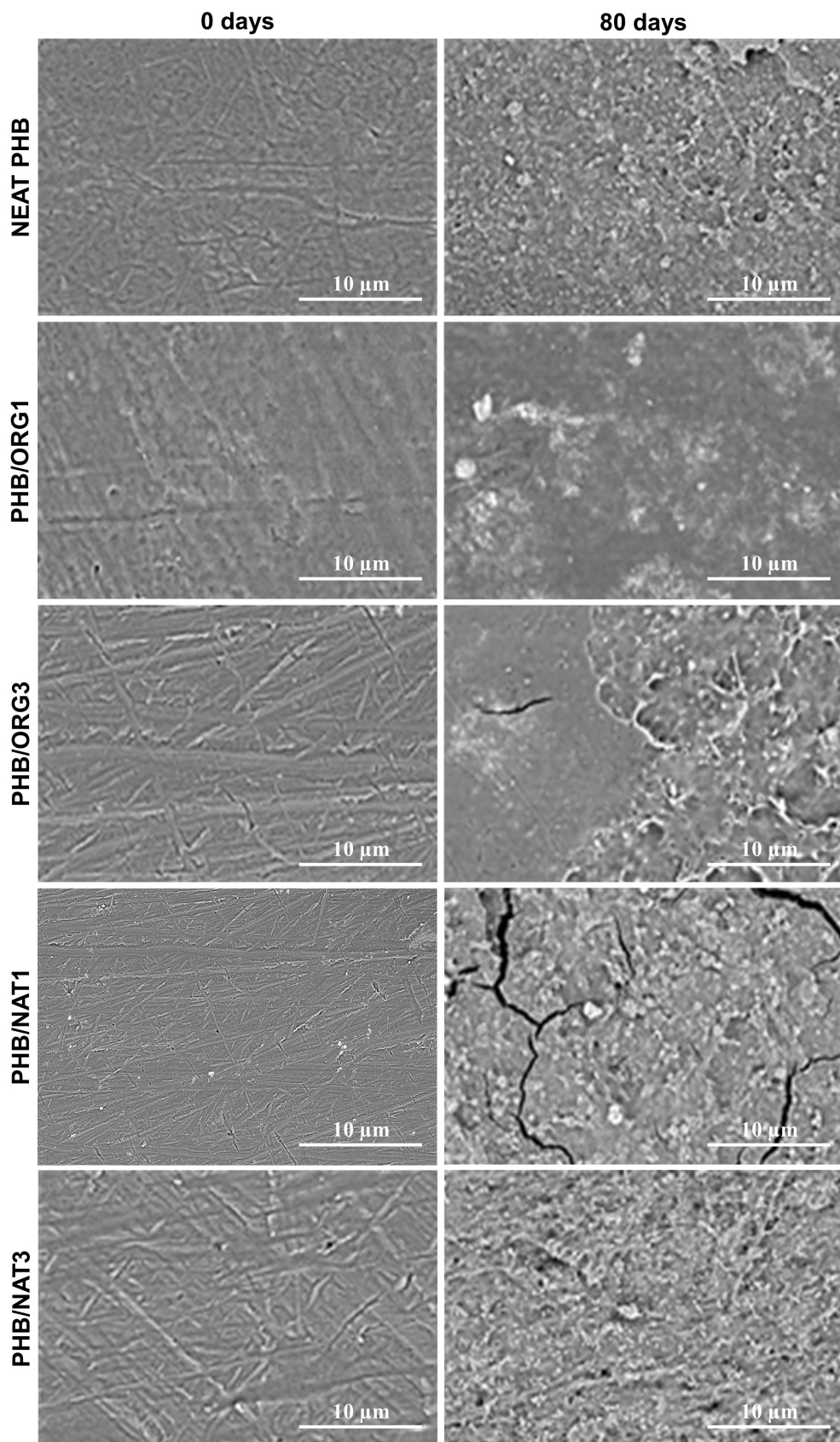


Figure 7. SEM micrographs of the systems before and after biodegradation.

Table 4. Microbial count values in colony forming units.

Time (days)	Colony Forming Units mL ⁻¹				
	PHB	NAT1	NAT3	ORG1	ORG3
0	3.6 (± 0.31) x10 ⁴	3.6 (± 0.18) x10 ⁴	3.6 (± 0.23) x10 ⁴	3.6 (± 0.27) x10 ⁴	3.6 (± 0.43) x10 ⁴
20	3.2 (± 0.28) x10 ³	2.9 (± 0.31) x10 ³	2.7 (± 0.28) x10 ³	2.5 (± 0.17) x10 ³	3.1 (± 0.13) x10 ³
40	2.1 (± 0.16) x10 ²	1.7 (± 0.19) x10 ²	1.8 (± 0.21) x10 ²	1.8 (± 0.32) x10 ²	1.9 (± 0.29) x10 ²
60	1.7 (± 0.28) x10 ²	1.1 (± 0.19) x10 ²	1.2 (± 0.41) x10 ²	1.4 (± 0.33) x10 ²	1.2 (± 0.27) x10 ²
80	7.6 (± 0.13) x10	6.5 (± 0.14) x10	7.0 (± 0.11) x10	5.7 (± 0.10) x10	6.3 (± 0.22) x10

Values indicated as: Mean (Standard Deviation).

Previously, PHB films attacked by microorganisms from the water of a river in the state of São Paulo (Brazil) were investigated²⁸, and films with a porous structure were observed after exposure to the biotreatment, suggesting the presence of material degradation. The superficial alterations of the materials due to the microbial action intensified the colonization of microorganisms, exposing the polymer to the contact of excreted enzymes that specifically attacked the carbonyl groups present in the polymeric matrix, this behavior has also been previously reported⁷².

3.5. Bacterial counting

It is observed that the highest bacterial count occurred in the neat PHB film, evincing that PHB constitutes a carbon source for microbial development²². The number of microorganisms in the different bionanocomposites tested was similar (Table 4), as all films have a high amount ($\geq 97\%$) of PHB. Faria and Martins-Franchetti²⁸ reported PHB biodegrades fairly rapidly compared to other polymers, which was taken as evidence that PHB is a good carbon source for the microbial growth.

During the biodegradation test, a gradual decrease in the number of microorganisms is observed, which was attributed to the reduction of the available carbon in the medium, as the bionanocomposites were degraded and the carbon consumed by the bacterial growth. There were no significant differences observed in the amounts of heterotrophic bacteria among the different bionanocomposite films investigated as a function of biodegradation time. It is believed that the reason for this nearly equivalent amounts in bacterial growth is the same source of bacteria and initial number of microorganisms employed as well as the similarities in composition of the bionanocomposite films tested.

3.6. Identification of the bacteria present in the biodegradation test

The identification and percentage of bacteria present in the liquid medium used for the biodegradation test is showed in Table 5. The bacteria in the biodegradation systems were identified at each withdrawal period by analyzing water samples and isolated colonies on Petrifilm membranes. To calculate the frequency value, the number of colonies of each species identified in all samples was considered.

The most frequent species found in the water biodegradation system of the Parnaíba River were *Pseudomonas aeruginosa* and *Pseudomonas putida*. About half (46.6%) of the analyzed samples belonged to the *Pseudomonas* genus, which is commonly found in aquatic environments⁸⁶.

Table 5. Identification of the bacteria present in the biodegradation systems.

Bacteria	Frequency (%)
<i>Pseudomonas aeruginosa</i>	28.3
<i>Pseudomonas putida</i>	18.3
<i>Stenotrophomonas maltophilia</i>	14.1
<i>Enterobacter cloacae</i>	11.6
<i>Yersinia enterocolitica</i>	8.3
<i>Aeromonas salmonicida</i>	7.5
<i>Brevundimonas diminuta</i>	6.6
<i>Rhizobium radiobacter</i>	5.0

Pseudomonas species are known to be opportunistic bacteria that can cause severe infections. *P. aeruginosa* is the most frequently involved species in infections affecting different organs, such as the respiratory tract, urinary tract, and bloodstream⁸⁷. Its ability to grow in nutritionally poor environments, with low levels of dissolved solids and organic compounds, confirms its adaptability. However, the presence of *Pseudomonas* in water for human consumption indicates contamination, and the current legislation establishes the absence of this microorganism or less than 1.0 CFU in 100 mL of water as a quality standard. The high incidence of *P. aeruginosa* in different environments can be attributed to its easy adaptation to environmental conditions, such as nutrition, temperature, and humidity⁸⁸. Several groups of bacteria, such as *Pseudomonas*, *Marinobacter*, *Alcanivorax*, *Microbulbifer*, *Sphingomonas*, *Micrococcus*, *Cellulomonas*, and *Gordonia*, are known for their ability to degrade alkane and aromatic hydrocarbons⁸⁹. In addition, *Pseudomonas lemoignei* has been shown to biodegrade PHB films in liquid medium⁷².

Pseudomonas aeruginosa and *Pseudomonas putida* are bacteria that can cause diseases in humans, particularly in those with compromised immune systems, although they can also be found naturally in the environment, such as in soils, water, and surfaces, without causing health problems for most healthy individuals. *Pseudomonas aeruginosa* is an opportunistic pathogen responsible for nosocomial infections, such as pneumonia, urinary tract infections, bloodstream infections, and wound infections, exhibiting antibiotic resistance mechanisms and the formation of resistant biofilms, making treatment more challenging. On the other hand, *Pseudomonas putida* is generally considered beneficial, playing a significant role in the biodegradation of organic compounds and the remediation of environmental pollutants, although, in very rare circumstances, it can cause infections in immunocompromised individuals⁹⁰⁻⁹².

Table 6. Biofilm formation at each withdrawal for each system analysed in duplicate.

Time (days)	PHB	ORG1	ORG3	NAT1	NAT3
20	+(2)	+(1)	+(2)	-	-
40	+(2)	+(1)	+(2)	-	+(1)
60	+(2)	+(2)	+(2)	+(2)	+(2)
80	+(2)	+(2)	+(2)	+(2)	+(2)

-: No biofilm; +(1): Biofilm present in one of the samples tested; +(2): Biofilm present in both samples tested.

Each film contained at least one identified bacteria sample, leading to the assumption that similarities in bacterial composition can be attributed to the shared aquatic medium and incubation conditions. Differences in sample composition were minimal, with a maximum filler amount of 3 wt%, resulting in at least 94.5% PHB in all samples.

Our data also indicates that the bacteria identified in the biodegradation systems are all Gram-negative bacilli, most of them considered opportunistic pathogens, and that their presence in the water is due to the pollution of said river. The species *Aeromonas salmonicida* is a fish pathogen rarely found in warm waters, and its isolation was not expected⁹³. The species *Brevibomonas diminuta* and *Stenotrophomonas maltophilia* are closely related to the genus *Pseudomonas*; they can be isolated from water, and the present enzymes are able to degrade polymers and other materials⁹⁴. Loredo-Treviño et al.⁹⁵ reported that the species *Pseudomonas putida* was able to degrade 92% of commercial polyurethane after incubation for 4 days at 25°C. We can state that the bacteria identified in the work were able to promote the degradation of the bionanocomposites tested.

However, it is noteworthy that according to the literature, specific bacteria with the ability to degrade PHAs may pose a risk to human health or other organisms if they experience widespread proliferation. Notable examples include *Pseudomonas aeruginosa* and *Bacillus subtilis*, which can induce infections in humans, particularly those with compromised immune systems. Furthermore, some species of *Streptomyces* spp. can cause infections in humans and animals, such as actinomycosis, while *Nocardia* spp. can lead to infections in humans and animals, including nocardiosis⁹⁶⁻⁹⁸.

3.7. Biofilm formed by *Pseudomonas aeruginosa*

The presence of biofilm by *Pseudomonas aeruginosa* adhered to the surface of the films in all bionanocomposites investigated in duplicate analysis is in Table 6.

Pandey et al.⁹⁹ reported that alginate, a polysaccharide polymer, gives bacteria a mucoid appearance that acts as mediator of adhesion to mucin, a fact proven in the films studied in this work that presented a mucous and gelatinous aspect, difficult to handle. Similarly, Kyaw et al.¹⁰⁰ reported that *Pseudomonas aeruginosa* bacteria exhibit a strong potential for degrading low-density polyethylene (LDPE) due to their ability to form a biofilm on the surface of this material in a short incubation period. The biofilm formation reduces the hydrophobicity of the polymer, allowing for accelerated degradation rates.

It is worth noting that the bionanocomposite PHB/ORG3 exhibited a composition that was highly conducive to the adhesion of biofilm formed by *Pseudomonas aeruginosa*.

Biofilm formation was observed in both of the analyzed films at all withdrawal times, similar to what occurred with neat PHB. The incorporation of 3 wt% of organophilic clay to PHB led to faster biofilm formation by *P. aeruginosa*. These results were consistent with those obtained through optical microscopy, where it was found that PHB/ORG3 was the film with the highest degree of degradation.

4. Conclusion

This study aimed to produce a PHB/clay bionanocomposite compatibilized with PP-g-MA, incorporating both intercalated and exfoliated structures, by employing a natural clay and an organophilic clay (Cloisite 20A). The obtained materials exhibited favorable and accelerated biodegradation properties. The predominant identification of *Pseudomonas* bacteria indicated their ability to depolymerize PHB in all tested systems, under the evaluated conditions. The presence of specific microorganisms is believed to reduce the resistance to degradation of biopolymer materials when exposed to contaminated water. Consequently, the resulting depolymerization process is expected to cause less environmental harm. In conclusion, the PHB/ORG3 film shows great potential as a promising alternative for the packaging industry.

5. Acknowledgments

The authors thank the Laboratory of Polymer and Conjugated Materials – LAPCON/UFPI to the physical structure, CNPq for financial support, Central Public Health Laboratory of Piauí (LACEN) and Med Imagem (Piauí, Brazil).

6. References

- Wang Y-W, Mo W, Yao H, Wu Q, Chen J, Chen G-Q. Biodegradation studies of poly(3-hydroxybutyrate-co-3-hydroxyhexanoate). Polym Degrad Stabil. 2004;85(2):815-21. <http://dx.doi.org/10.1016/j.polymdegradstab.2004.02.010>.
- Zhou W, Bergsma S, Colpa DI, Euverink G-JW, Krooneman J. Polyhydroxalkanoates (PHAs) synthesis and degradation by microbes and applications towards a circular economy. J Environ Manage. 2023;341:118033. <http://dx.doi.org/10.1016/j.jenvman.2023.118033>.
- Eraslan K, Aversa C, Nofar M, Barletta M, Gisario A, Salehiyan R, et al. Poly(3-hydroxybutyrate-co-3-hydroxyhexanoate) (PHBH): synthesis, properties, and applications - a review. Eur Polym J. 2022;167:111044. <http://dx.doi.org/10.1016/j.eurpolymj.2022.111044>.
- Baidurah S, Kobayashi T, Aziz AA. PLA based plastics for enhanced sustainability of the environment. In: Hashmi MSJ, editor. Encyclopedia of materials: plastics and polymers. Oxford: Elsevier; 2022. p. 511-9. <http://dx.doi.org/10.1016/B978-0-12-820352-1.00175-9>.

5. Shekarchizadeh H, Nazeri FS. Active nanoenabled packaging for the beverage industry. In: Amrane A, Rajendran S, Nguyen TA, Assadi AA, Sharoba AM, editors. *Nanotechnology in the beverage industry*. Cambridge: Elsevier; 2020. p. 587-607. <http://dx.doi.org/10.1016/B978-0-12-819941-1.00020-1>.
6. Amir M, N Bano, MR Zaheer, T Haq, Roohi. Impact of biodegradable packaging materials on food quality: a sustainable approach. In: Inamuddin I, Altalhi T, editors. *Biodegradable materials and their applications*. New Jersey: John Wiley & Sons; 2022. p. 627-52. <http://dx.doi.org/10.1002/9781119905301.ch22>.
7. Cañado N, Lizundia E, Akizu-Gardoki O, Minguez R, Lekube B, Arrillaga A, et al. 3D printing to enable the reuse of marine plastic waste with reduced environmental impacts. *J Ind Ecol*. 2022;26(6):2092-107. <http://dx.doi.org/10.1111/jiec.13302>.
8. Bao Q, Wong W, Liu S, Tao X. Accelerated degradation of poly(lactide acid)/poly(hydroxybutyrate) (PLA/PHB) yarns/fabrics by UV and O₂ exposure in South China seawater. *Polymers*. 2022;14(6):1216. <http://dx.doi.org/10.3390/polym14061216>.
9. Yue C, Huo M, Li H, Liu Y, Xu M, Song Y. Printability, shape-memory, and mechanical properties of PHB/PCL/CNFs composites. *J Appl Polym Sci*. 2021;138(22):50510. <http://dx.doi.org/10.1002/app.50510>.
10. Bokrova J, Marova I, Matouskova P, Pavelkova R. Fabrication of novel PHB-liposome nanoparticles and study of their toxicity in vitro. *J Nanopart Res*. 2019;21(3):49. <http://dx.doi.org/10.1007/s11051-019-4484-7>.
11. Yeo JCC, Muiruri JK, Thitsartarn W, Li Z, He C. Recent advances in the development of biodegradable PHB-based toughening materials: approaches, advantages and applications. *Mater Sci Eng C*. 2018;92:1092-116. <http://dx.doi.org/10.1016/j.msec.2017.11.006>.
12. Zhong Y, Godwin P, Jin Y, Xiao H. Biodegradable polymers and green-based antimicrobial packaging materials: a mini-review. *Adv Ind Eng Polym Res*. 2020;3(1):27-35. <http://dx.doi.org/10.1016/j.aiepr.2019.11.002>.
13. Calvino C, Macke N, Kato R, Rowan SJ. Development, processing and applications of bio-sourced cellulose nanocrystal composites. *Prog Polym Sci*. 2020;103:101221. <http://dx.doi.org/10.1016/j.progpolymsci.2020.101221>.
14. Kwon S, Zambrano MC, Pawlak JJ, Ford E, Venditti RA. Aquatic biodegradation of poly(β -hydroxybutyrate) and polypropylene blends with compatibilizer and the generation of micro- and nano-plastics on biodegradation. *J Polym Environ*. 2023;31(8):3619-31. <http://dx.doi.org/10.1007/s10924-023-02832-y>.
15. Utracki LA. *Clay-containing polymeric nanocomposites*. Shawbury, UK: RAPRA Technology; 2004.
16. Ray SS, Okamoto M. Polymer/layered silicate nanocomposites: a review from preparation to processing. *Prog Polym Sci*. 2003;28(11):1539-641. <http://dx.doi.org/10.1016/j.progpolymsci.2003.08.002>.
17. Bai Z, Dou Q. Rheology, morphology, crystallization behaviors, mechanical and thermal properties of poly(lactic acid)/polypropylene/maleic anhydride-grafted polypropylene blends. *J Polym Environ*. 2018;26(3):959-69. <http://dx.doi.org/10.1007/s10924-017-1006-5>.
18. Oliveira RRD, Oliveira TAD, Silva LRCD, Barbosa R, Alves TS, Carvalho LHD, et al. Effect of reprocessing cycles on the morphology and mechanical properties of a poly(propylene)/poly(hydroxybutyrate) blend and its nanocomposite. *Mater Res*. 2021;24(4):e20200372. <http://dx.doi.org/10.1590/1980-5373-mr-2020-0372>.
19. Darder M, Aranda P, Ruiz-Hitzky E. Bionanocomposites: a new concept of ecological, bioinspired, and functional hybrid. *Adv Mater*. 2007;19(10):1309-19. <http://dx.doi.org/10.1002/adma.200602328>.
20. Ahmed T, Shahid M, Azeem F, Rasul I, Shah AA, Noman M, et al. Biodegradation of plastics: current scenario and future prospects for environmental safety. *Environ Sci Pollut Res Int*. 2018;25(8):7287-98. <http://dx.doi.org/10.1007/s11356-018-1234-9>.
21. Ublekov F, Budurova D, Staneva M, Natova M, Penchev H. Self-supporting electrospun PHB and PHBV/organoclay nanocomposite fibrous scaffolds. *Mater Lett*. 2018;218:353-6. <http://dx.doi.org/10.1016/j.matlet.2018.02.056>.
22. Shimao M. Biodegradation of plastics. *Curr Opin Biotechnol*. 2001;12(3):242-7. [http://dx.doi.org/10.1016/S0958-1669\(00\)00206-8](http://dx.doi.org/10.1016/S0958-1669(00)00206-8).
23. Sinha Ray S, Bousmina M. Biodegradable polymers and their layered silicate nanocomposites: in greening the 21st century materials world. *Prog Mater Sci*. 2005;50(8):962-1079. <http://dx.doi.org/10.1016/j.pmatsci.2005.05.002>.
24. Voicu SI, Condruz RM, Mitrani V, Cimpean A, Miculescu F, Andronescu C, et al. Sericin covalent immobilization onto cellulose acetate membrane for biomedical applications. *ACS Sustain Chem& Eng*. 2016;4(3):1765-74. <http://dx.doi.org/10.1021/acssuschemeng.5b01756>.
25. Nezha Tahri J, Wifak B, Hanane S, Naïma El G. Biodegradation: involved microorganisms and genetically engineered microorganisms. In: Chamy R, Rosenkranz F, editors. *Biodegradation*. Rijeka: IntechOpen; 2013. p. 289-320. <http://dx.doi.org/10.5772/56194>.
26. Volova TG, Boyandin AN, Vasiliiev AD, Karpov VA, Prudnikova SV, Mishukova OV, et al. Biodegradation of polyhydroxylalkanoates (PHAs) in tropical coastal waters and identification of PHA-degrading bacteria. *Polym Degrad Stabil*. 2010;95(12):2350-9. <http://dx.doi.org/10.1016/j.polymdegradstab.2010.08.023>.
27. Volova TG, Prudnikova SV, Vinogradova ON, Syrvacheva DA, Shishatskaya EI. Microbial degradation of polyhydroxylalkanoates with different chemical compositions and their biodegradability. *Microb Ecol*. 2017;73(2):353-67. <http://dx.doi.org/10.1007/s00248-016-0852-3>.
28. Faria AUD, Martins-Franchetti SM. Biodegradação de filmes de polipropileno (PP), poli (3-hidroxibutirato)(PHB) e blenda de PP/PHB por microrganismos das águas do Rio Atibaia. *Polímeros*. 2010;20(2):141-7. <http://dx.doi.org/10.1590/S0104-14282010005000024>.
29. Sayyed RZ, Wani SJ, Alarfaj AA, Syed A, El-Enshasy HA. Production, purification and evaluation of biodegradation potential of PHB depolymerase of *Stenotrophomonas* sp. RZS7. *PLoS One*. 2020;15(1):e0220095. <http://dx.doi.org/10.1371/journal.pone.0220095>.
30. Atlas RM. *Handbook of microbiological media*. Leiden: CRC Press; 2004. <http://dx.doi.org/10.1201/9781420039726>.
31. Araque LM, Morais ACL, Alves TS, Azevedo JB, Carvalho LH, Barbosa R. Preparation and characterization of poly(hydroxybutyrate) and hollow glass microspheres composite films: morphological, thermal, and mechanical properties. *J Mater Res Technol*. 2019;8(1):935-43. <http://dx.doi.org/10.1016/j.jmrt.2018.07.005>.
32. Fu S, Sun Z, Huang P, Li Y, Hu N. Some basic aspects of polymer nanocomposites: a critical review. *Nano Materials Science*. 2019;1(1):2-30. <http://dx.doi.org/10.1016/j.nanoms.2019.02.006>.
33. Almeida VO, Batista KA, Di-Medeiros MCB, Moraes MG, Fernandes KF. Effect of drought stress on the morphological and physicochemical properties of starches from *Trimezia juncifolia*. *Carbohydr Polym*. 2019;212:304-11. <http://dx.doi.org/10.1016/j.carbpol.2019.02.015>.
34. Silva N, Taniwaki MH, Junqueira VC, Silveira N, Okazaki MM, Gomes RAR. *Microbiological examination methods of food and water: a laboratory manual*. 2nd ed. Leiden: CRC Press; 2018.
35. Koneman EW. *Koneman's color atlas and textbook of diagnostic microbiology*. 7th ed. Philadelphia: Wolters Kluwer; 2017.
36. Žiemytė M, Carda-Díéguez M, Rodríguez-Díaz JC, Ventero MP, Mira A, Ferrer MD. Real-time monitoring of *Pseudomonas aeruginosa* biofilm growth dynamics and persister cells' eradication. *Emerg Microbes Infect*. 2021;10(1):2062-75. <http://dx.doi.org/10.1080/22221751.2021.1994355>.
37. Paiva LB, Morales AR, Díaz FRV. Organophilic clays: characteristics, preparation methods, intercalation compounds and characterization techniques. *Ceramica*. 2008;54:213-26. <http://dx.doi.org/10.1590/S0366-69132008000200012>.

38. Szazdi L, Pozsgay A, Pukanszky B. Factors and processes influencing the reinforcing effect of layered silicates in polymer nanocomposites. *Eur Polym J.* 2007;43(2):345-59. <http://dx.doi.org/10.1016/j.eurpolymj.2006.11.005>.
39. Mekhzoum MEM, Raji M, Rodrigue D, Qaiss A, Bouhfid R. The effect of benzothiazolium surfactant modified montmorillonite content on the properties of polyamide 6 nanocomposites. *Appl Clay Sci.* 2020;185:105417. <http://dx.doi.org/10.1016/j.clay.2019.105417>.
40. Bee S-L, Abdullah MAA, Mamat M, Bee S-T, Sin LT, Hui D, et al. Characterization of silylated modified clay nanoparticles and its functionality in PMMA. *Compos, Part B Eng.* 2017;110:83-95. <http://dx.doi.org/10.1016/j.compositesb.2016.10.084>.
41. Ma H, Wei Z, Zhou S, Zhu H, Tang J, Yin J, et al. Supernucleation, crystalline structure and thermal stability of bacterially synthesized poly(3-hydroxybutyrate) polyester tailored by thymine as a biocompatible nucleating agent. *Int J Biol Macromol.* 2020;165:1562-73. <http://dx.doi.org/10.1016/j.ijbiomac.2020.10.044>.
42. Sousa RR Jr, Santos CAS, Ito NM, Suqueira AN, Lackner M, Santos DJ. PHB processability and property improvement with linear-chain polyester oligomers used as plasticizers. *Polymers.* 2022;14(19):4197. <http://dx.doi.org/10.3390/polym14194197>.
43. Garrido-Miranda KA, Rivas BL, Pérez MA. Poly(3-hydroxybutyrate)-thermoplastic starch-organoclay bionanocomposites: surface properties. *J Appl Polym Sci.* 2017;134(34):45217. <http://dx.doi.org/10.1002/app.45217>.
44. Abbasi F, Tavakoli A, Razavi Aghjeh MK. Rheology, morphology, and mechanical properties of reactive compatibilized polypropylene/polystyrene blends via Friedel-Crafts alkylation reaction in the presence of clay. *Journal of Vinyl and Additive Technology.* 2018;24(1):18-26. <http://dx.doi.org/10.1002/vnl.21522>.
45. Guarás MP, Alvarez VA, Ludueña LN. Biodegradable nanocomposites based on starch/polycaprolactone/compatibilizer ternary blends reinforced with natural and organo-modified montmorillonite. *J Appl Polym Sci.* 2016;133(44):44163. <http://dx.doi.org/10.1002/app.44163>.
46. Othman N, Hassan A, Razak Rahmat A, Uzir Wahit M. Effect of compatibilizer type on properties of 70: 30 polyamide 6/polypropylene/MMT nanocomposites. *Int J Polym Mater.* 2007;56(9):893-909. <http://dx.doi.org/10.1080/00914030601123377>.
47. Sandhya PK, Sreekala MS, Thomas S. Biopolymer-based blend nanocomposites. In: Thomas S, Ar A, Chirayil J, Thomas B, editors. *Handbook of biopolymers.* Singapore: Springer Nature Singapore; 2022. p. 1-28. http://dx.doi.org/10.1007/978-981-16-6603-2_20-1.
48. Souza VGL, Pires JRA, Rodrigues PF, Lopes AAS, Fernandes FMB, Duarte MP, et al. Bionanocomposites of chitosan/montmorillonite incorporated with Rosmarinus officinalis essential oil: development and physical characterization. *Food Packag Shelf Life.* 2018;16:148-56. <http://dx.doi.org/10.1016/j.fpsl.2018.03.009>.
49. Silva RDN, Silva LRC, Moraes ACL, Alves TS, Barbosa R. Study of the hydrolytic degradation of poly-3-hydroxybutyrate in the development of blends and polymeric bionanocomposites. *Journal of Thermoplastic Composite Materials.* 2021;34(7):884-901. <http://dx.doi.org/10.1177/0892705719856044>.
50. Zare Y. Study of nanoparticles aggregation/agglomeration in polymer particulate nanocomposites by mechanical properties. *Compos, Part A Appl Sci Manuf.* 2016;84:158-64. <http://dx.doi.org/10.1016/j.compositesa.2016.01.020>.
51. Jin T-X, Liu C, Zhou M, Chai S, Chen F, Fu Q. Crystallization, mechanical performance and hydrolytic degradation of poly (butylene succinate)/graphene oxide nanocomposites obtained via in situ polymerization. *Compos, Part A Appl Sci Manuf.* 2015;68:193-201. <http://dx.doi.org/10.1016/j.compositesa.2014.09.025>.
52. Janowski G, Frącz W, Bąk Ł, Trzepieciński T. The effect of the extrusion method on processing and selected properties of Poly (3-hydroxybutyric-co-3-hydroxyvaleric Acid)-based biocomposites with flax and hemp fibers. *Polymers.* 2022;14(24):5370. <http://dx.doi.org/10.3390/polym14245370>.
53. Rajan KP, Thomas SP, Gopanna A, Chavali M. Polyhydroxybutyrate (PHB): a standout biopolymer for environmental sustainability. In: Martínez LMT, Kharissova OV, Kharisov BI, editors *Handbook of ecomaterials.* Cham: Springer International Publishing; 2017. p. 1-23.
54. Bittmann B, Bouza R, Barral L, Diez J, Ramirez C. Poly (3-hydroxybutyrate-co-3-hydroxyvalerate)/clay nanocomposites for replacement of mineral oil based materials. *Polym Compos.* 2013;34(7):1033-40. <http://dx.doi.org/10.1002/pc.22510>.
55. Zhu J, Abeykoon C, Karim N. Investigation into the effects of fillers in polymer processing. *Int J Lightweight Mater Manuf.* 2021;4(3):370-82. <http://dx.doi.org/10.1016/j.ijlmm.2021.04.003>.
56. Vieira IRS, Costa LFO, Miranda GS, Nardeechia S, Monteiro MSSB, Ricci-Júnior E, et al. Waterborne poly(urethane-urea)s nanocomposites reinforced with clay, reduced graphene oxide and respective hybrids: synthesis, stability and structural characterization. *J Polym Environ.* 2020;28(1):74-90. <http://dx.doi.org/10.1007/s10924-019-01584-y>.
57. Fambri L, Dorigato A, Pegoretti A. Role of surface-treated silica nanoparticles on the thermo-mechanical behavior of poly(lactide). *Appl Sci.* 2020;10(19):6731. <http://dx.doi.org/10.3390/app10196731>.
58. Valle Julianelli GC, David GDS, Santos TN, Sebastiao PJO, Tavares MIB. Influence of TiO₂ nanoparticle on the thermal, morphological and molecular characteristics of PHB matrix. *Polym Test.* 2018;65:156-62. <http://dx.doi.org/10.1016/j.polymertesting.2017.11.018>.
59. Ankush K, Pugazhenthi G, Mohit K, Vasanth D. Experimental study on fabrication, biocompatibility and mechanical characterization of polyhydroxybutyrate-ball clay bionanocomposites for bone tissue engineering. *Int J Biol Macromol.* 2022;209:1995-2008. <http://dx.doi.org/10.1016/j.ijbiomac.2022.04.178>.
60. Vahabi H, Michely L, Moradkhani G, Akbari V, Cochez M, Vagner C, et al. Thermal stability and flammability behavior of poly(3-hydroxybutyrate) (PHB) based composites. *Materials.* 2019;12(14):2239. <http://dx.doi.org/10.3390/ma12142239>.
61. Fonseca FMC, Patrício PSO, Souza SD, Oréfice RL. Prodegradant effect of titanium dioxide nanoparticulates on polypropylene-polyhydroxybutyrate blends. *J Appl Polym Sci.* 2018;135(33):46636. <http://dx.doi.org/10.1002/app.46636>.
62. Lee J-H, Jung D, Hong C-E, Rhee KY, Advani SG. Properties of polyethylene-layered silicate nanocomposites prepared by melt intercalation with a PP-g-MA compatibilizer. *Compos Sci Technol.* 2005;65(13):1996-2002. <http://dx.doi.org/10.1016/j.compscitech.2005.03.015>.
63. Kervran M, Vagner C, Cochez M, Ponçot M, Saeb MR, Vahabi H. Thermal degradation of polylactic acid (PLA)/polyhydroxybutyrate (PHB) blends: a systematic review. *Polym Degrad Stabil.* 2022;201:109995. <http://dx.doi.org/10.1016/j.polymdegradstab.2022.109995>.
64. Pessini P, Daitx TS, Ferreira CI, Mauler RS. Selective localization of organophilic clay Cloisite 30B in biodegradable poly(lactic acid)/poly(3-hydroxybutyrate) blends. *J Appl Polym Sci.* 2021;138(40):51175. <http://dx.doi.org/10.1002/app.51175>.
65. Silva RM Jr, Oliveira TA, Araque LM, Alves TS, Carvalho LH, Barbosa R. Thermal behavior of biodegradable bionanocomposites: influence of bentonite and vermiculite clays. *J Mater Res Technol.* 2019;8(3):3234-43. <http://dx.doi.org/10.1016/j.jmrt.2019.05.011>.
66. Chen B, Cai D, Luo Z, Chen C, Zhang C, Qin P, et al. Corn cob residual reinforced polyethylene composites considering the biorefinery process and the enhancement of performance. *J Clean Prod.* 2018;198:452-62. <http://dx.doi.org/10.1016/j.jclepro.2018.07.080>.
67. Souza JDL, Chiaregato CG, Faiez R. Green composite based on PHB and montmorillonite for KNO₃ and NPK delivery system. *J Polym Environ.* 2018;26(2):670-9. <http://dx.doi.org/10.1007/s10924-017-0979-4>.
68. Budhiraja V, Urh A, Horvat P, Krzan A. Synergistic adsorption of organic pollutants on weathered polyethylene microplastics. *Polymers.* 2022;14(13):2674. <http://dx.doi.org/10.3390/polym14132674>.

69. Mamat MRZ, Ariffin H, Hassan MA, Mohd Zahari MAK. Bio-based production of crotonic acid by pyrolysis of poly (3-hydroxybutyrate) inclusions. *J Clean Prod.* 2014;83:463-72. <http://dx.doi.org/10.1016/j.jclepro.2014.07.064>.
70. Xiang H, Wen X, Miu X, Li Y, Zhou Z, Zhu M. Thermal depolymerization mechanisms of poly(3-hydroxybutyrate-co-3-hydroxyvalerate). *Prog Nat Sci.* 2016;26(1):58-64. <http://dx.doi.org/10.1016/j.pnsc.2016.01.007>.
71. Elhami V, Hempenius MA, Schuur B. Crotonic acid production by pyrolysis and vapor fractionation of mixed microbial culture-based poly(3-hydroxybutyrate-co-3-hydroxyvalerate). *Ind Eng Chem Res.* 2023;62(2):916-23. <http://dx.doi.org/10.1021/acs.iecr.2c03791>.
72. Spyros A, Kimmich R, Briese BH, Jendrossek D. H NMR imaging study of enzymatic degradation in poly (3-hydroxybutyrate) and poly (3-hydroxybutyrate-co-3-hydroxyvalerate): evidence for preferential degradation of the amorphous phase by PHB depolymerase B from *Pseudomonas lemoignei*. *Macromolecules.* 1997;30(26):8218-25. <http://dx.doi.org/10.1021/ma971193m>.
73. Camani PH, Toguchi JPM, Fiori APS, Rosa DS. Impact of unmodified (PGV) and modified (Cloisite20A) nanoclays into biodegradability and other properties of (bio) nanocomposites. *Appl Clay Sci.* 2020;186:105453. <http://dx.doi.org/10.1016/j.clay.2020.105453>.
74. Rummel CD, Jahnke A, Gorokhova E, Kühnel D, Schmitt-Jansen M. Impacts of biofilm formation on the fate and potential effects of microplastic in the aquatic environment. *Environ Sci Technol Lett.* 2017;4(7):258-67. <http://dx.doi.org/10.1021/acs.estlett.7b00164>.
75. Roohi, Zaheer MR, Kuddus M. PHB (poly- β -hydroxybutyrate) and its enzymatic degradation. *Polym Adv Technol.* 2018;29(1):30-40. <http://dx.doi.org/10.1002/pat.4126>.
76. Li R, Yang J, Xiao Y, Long L. In vivo immobilization of an organophosphorus hydrolyzing enzyme on bacterial polyhydroxyalkanoate nano-granules. *Microb Cell Fact.* 2019;18(1):166. <http://dx.doi.org/10.1186/s12934-019-1201-2>.
77. Kumar M, Rathour R, Singh R, Sun Y, Pandey A, Gnansounou E, et al. Bacterial polyhydroxyalkanoates: opportunities, challenges, and prospects. *J Clean Prod.* 2020;263:121500. <http://dx.doi.org/10.1016/j.jclepro.2020.121500>.
78. Bher A, Mayekar PC, Auras RA, Schvezov CE. Biodegradation of biodegradable polymers in mesophilic aerobic environments. *Int J Mol Sci.* 2022;23(20):12165. <http://dx.doi.org/10.3390/ijms232012165>.
79. Al-Hawash AB, Dragh MA, Li S, Alhujaily A, Abbood HA, Zhang X, et al. Principles of microbial degradation of petroleum hydrocarbons in the environment. *Egypt J Aquat Res.* 2018;44(2):71-6. <http://dx.doi.org/10.1016/j.ejar.2018.06.001>.
80. Amobonye A, Bhagwat P, Singh S, Pillai S. Plastic biodegradation: frontline microbes and their enzymes. *Sci Total Environ.* 2021;759:143536. <http://dx.doi.org/10.1016/j.scitotenv.2020.143536>.
81. Elumalai P, Parthipan P, Huang M, Muthukumar B, Cheng L, Govarthanan M, et al. Enhanced biodegradation of hydrophobic organic pollutants by the bacterial consortium: impact of enzymes and biosurfactants. *Environ Pollut.* 2021;289:117956. <http://dx.doi.org/10.1016/j.envpol.2021.117956>.
82. Shah AA, Hasan F, Hameed A, Ahmed S. Biological degradation of plastics: a comprehensive review. *Biotechnol Adv.* 2008;26(3):246-65. <http://dx.doi.org/10.1016/j.biotechadv.2007.12.005>.
83. Vasudeo Rane A, Kanny K, Abitha VK, Patil SS, Thomas S. Clay-polymer composites: design of clay polymer nanocomposite by mixing. In: Jlassi K, Chehimi MM, Thomas S, editors. *Clay-polymer nanocomposites.* Amsterdam: Elsevier; 2017. p. 113-44. <http://dx.doi.org/10.1016/B978-0-323-46153-5.00004-5>.
84. Larrañaga A, Lizundia E. A review on the thermomechanical properties and biodegradation behaviour of polyesters. *Eur Polym J.* 2019;121:109296. <http://dx.doi.org/10.1016/j.eurpolymj.2019.109296>.
85. Yuan J, Ma J, Sun Y, Zhou T, Zhao Y, Yu F. Microbial degradation and other environmental aspects of microplastics/plastics. *Sci Total Environ.* 2020;715:136968. <http://dx.doi.org/10.1016/j.scitotenv.2020.136968>.
86. Crone S, Vives-Florez M, Kvich L, Saunders AM, Malone M, Nicolaisen MH, et al. The environmental occurrence of *Pseudomonas aeruginosa*. *Acta Pathol Microbiol Scand Suppl.* 2020;128(3):220-31. <http://dx.doi.org/10.1111/apm.13010>.
87. Cristina ML, Sartini M, Schinca E, Ottria G, Casini B, Spagnolo AM. Evaluation of multidrug-resistant *P. aeruginosa* in healthcare facility water systems. *Antibiotics.* 2021;10(12):1500. <http://dx.doi.org/10.3390/antibiotics10121500>.
88. Pachori P, Gothwal R, Gandhi P. Emergence of antibiotic resistance *Pseudomonas aeruginosa* in intensive care unit: a critical review. *Genes Dis.* 2019;6(2):109-19. <http://dx.doi.org/10.1016/j.gendis.2019.04.001>.
89. Dashti N, Ali N, Salama S, Khanafar M, Al-Shamy G, Al-Awadhi H, et al. Culture-independent analysis of hydrocarbonoclastic bacterial communities in environmental samples during oil-bioremediation. *MicrobiologyOpen.* 2019;8(2):e00630. <http://dx.doi.org/10.1002/mbo3.630>.
90. Ruiz-Roldán L, Rojo-Bezares B, de Toro M, López M, Toledano P, Lozano C, et al. Antimicrobial resistance and virulence of *Pseudomonas* spp. among healthy animals: concern about exolysin ExlA detection. *Sci Rep.* 2020;10(1):11667. <http://dx.doi.org/10.1038/s41598-020-68575-1>.
91. Schito AM, Piatti G, Caviglia D, Zuccari G, Zorzoli A, Marimpietri D, et al. Bactericidal activity of non-cytotoxic cationic nanoparticles against clinically and environmentally relevant *Pseudomonas* spp. isolates. *Pharmaceutics.* 2021;13(9):1411. <http://dx.doi.org/10.3390/pharmaceutics13091411>.
92. Urgancı NN, Yılmaz N, Alaşalvar GK, Yıldırım Z. *Pseudomonas aeruginosa* and its pathogenicity. *Turkish Journal of Agriculture-Food Science Technology.* 2022;10(4):726-38. <http://dx.doi.org/10.24925/turjaf.v10i4.726-738.4986>.
93. Fernández-Bravo A, Figueras MJ. An update on the genus aeromonas: taxonomy, epidemiology, and pathogenicity. *Microorganisms.* 2020;8(1):129. <http://dx.doi.org/10.3390/microorganisms8010129>.
94. Kolmakova OV, Gladyshev MI, Fonvielle JA, Ganzert L, Hornick T, Grossart H-P. Effects of zooplankton carcasses degradation on freshwater bacterial community composition and implications for carbon cycling. *Environ Microbiol.* 2019;21(1):34-49. <http://dx.doi.org/10.1111/1462-2920.14418>.
95. Loredo-Treviño A, Gutiérrez-Sánchez G, Rodríguez-Herrera R, Aguilar CN. Microbial enzymes involved in polyurethane biodegradation: a review. *J Polym Environ.* 2012;20(1):258-65. <http://dx.doi.org/10.1007/s10924-011-0390-5>.
96. Rathika R, Janaki V, Shanthi K, Kamala-Kannan S. Bioconversion of agro-industrial effluents for polyhydroxyalkanoates production using *Bacillus subtilis* RS1. *Int J Environ Sci Technol.* 2019;16(10):5725-34. <http://dx.doi.org/10.1007/s13762-018-2155-3>.
97. Cho JY, Lee Park S, Lee H-J, Kim SH, Suh MJ, Ham S, et al. Polyhydroxyalkanoates (PHAs) degradation by the newly isolated marine *Bacillus* sp. JY14. *Chemosphere.* 2021;283:131172. <http://dx.doi.org/10.1016/j.chemosphere.2021.131172>.
98. Di J, Chu Z, Zhang S, Huang J, Du H, Wei Q. Evaluation of the potential probiotic *Bacillus subtilis* isolated from two ancient sturgeons on growth performance, serum immunity and disease resistance of *Acipenser dabryanus*. *Fish Shellfish Immunol.* 2019;93:711-9. <http://dx.doi.org/10.1016/j.fsi.2019.08.020>.
99. Pandey S, Delgado C, Kumari H, Florez L, Mathee K. Outer-membrane protein LptD (PA0595) plays a role in the regulation of alginate synthesis in *Pseudomonas aeruginosa*. *J Med Microbiol.* 2018;67(8):1139-56. <http://dx.doi.org/10.1099/jmm.0.000752>.
100. Kyaw BM, Champakalakshmi R, Sakarkar MK, Lim CS, Sakarkar KR. Biodegradation of low density polyethylene (LDPE) by *Pseudomonas* species. *Indian J Microbiol.* 2012;52(3):411-9. <http://dx.doi.org/10.1007/s12088-012-0250-6>.